Dalton Transactions

Accepted Manuscript

This article can be cited before page numbers have been issued, to do this please use: A. R. Chakravarty, M. K. Raza, K. Mitra, A. Shettar, U. Basu and P. Kondaiah, *Dalton Trans.*, 2016, DOI: 10.1039/C6DT02590K.

This is an *Accepted Manuscript*, which has been through the Royal Society of Chemistry peer review process and has been accepted for publication.

Accepted Manuscripts are published online shortly after acceptance, before technical editing, formatting and proof reading. Using this free service, authors can make their results available to the community, in citable form, before we publish the edited article. We will replace this *Accepted Manuscript* with the edited and formatted *Advance Article* as soon as it is available.

You can find more information about *Accepted Manuscripts* in the Information for Authors.

Please note that technical editing may introduce minor changes to the text and/or graphics, which may alter content. The journal's standard Terms & Conditions and the Ethical guidelines still apply. In no event shall the Royal Society of Chemistry be held responsible for any errors or omissions in this *Accepted Manuscript* or any consequences arising from the use of any information it contains.

ROYAL SOCIETY OF CHEMISTRY

www.rsc.org/dalton

Journal Name

View Article Online
DOI: 10.1039/C6DT02590K

ARTICLE

Photoactive platinum(II) β-diketonates as dual action anticancer agents†

Received 00th January 20xx,
Accepted 00th January 20xx

DOI: 10.1039/x0xx00000x

www.rsc.org/

Md Kausar Raza[a,#], Koushambi Mitra[a,#], Abhijith Shettar[b], Uttara Basu[a], Paturu Kondaiah*[,b] and Akhil R. Chakravarty*[,a]

Platinum(II) complexes, viz. [Pt(L)(cur)] (**1**), [Pt(L)(py-acac)] (**2**) and [Pt(L)(an-acac)] (**3**), where HL is 4,4'-bis-dimethoxyazobenzene, Hcur is curcumin, Hpy-acac and Han-acac are pyrenyl and anthracenyl appended acetylacetone, were prepared, characterized and their anticancer activity studied. Complex [Pt(L)(acac)] (**4**) was used as a control. Complex **1** showed an absorption band at 430 nm (ε = 8.8 x 10^4 M^{-1} cm^{-1}). The anthracenyl and pyrenyl complexes displayed bands near 390 nm (ε = 3.7 x 10^4 for **3** and 4.4 x 10^4 M^{-1} cm^{-1} for **2**). Complex **1** showed an emission band at 525 nm (Φ = 0.017) in 10% DMSO-DPBS (pH, 7.2), while **2** and **3** were blue emissive (λ_{em} = 440 and 435, Φ = 0.058 and 0.045). There was an enhancement in emission intensity on glutathione (GSH) addition indicating diketonate release. The platinum(II) species thus formed acted as transcription inhibitor. The released β-diketonate base showed photo-chemotherapeutic activity. The complexes photocleaved plasmid DNA in blue light of 457 nm forming ~75% nicked circular (NC) DNA with hydroxyl radicals and singlet oxygen as the ROS. Complexes **1**-**3** were photocytotoxic in skin keratinocyte HaCaT cells giving IC_{50} of 8-14 μM in visible light (400-700 nm, 10 *J* cm^{-2}), while being non-toxic in the dark (IC_{50}: ~60 μM). Complex **4** was inactive. Complexes **1**-**3** generating cellular ROS caused apoptotic cell death in visible light as evidenced from DCFDA and annexin-V/FITC-PI assays. This work presents a novel way to deliver an active platinum(II) species and a phototoxic β-diketone species in the cancer cells.

Introduction

Cisplatin, oxaliplatin and carboplatin are the platinum-based compounds currently used as chemotherapeutic agents for a variety of cancers. The drug activity is related to the release of the labile ligands with concomitant generation of active platinum(II) species that acts as DNA crosslinker with transcription inhibition properties.[1-5] Cisplatin suffers from its reduced activity due to rapid loss of the chloride ligands in an intracellular medium and thus getting deactivated.[6] The rate of intracellular ligand release is relatively slow when the chlorides are substituted by a dianionic dicarboxylate in carboplatin or an oxalate ligand in oxaliplatin.[7,8] This leads to an enhancement of the drug activity. Despite their successful clinical use, these drugs suffer from several side effects. Photodynamic therapy (PDT) has emerged as an alternate non-invasive therapeutic method for treatment of several forms of cancer.[9,10] Platinum(II) β-diketonates with the ligands acting as good leaving group are known to show anticancer activity with transcription inhibition properties and improved aqueous solubility, hydrolytic stability, and cellular uptake.[11,12] The platinum(II) drugs are extracellular charge neutral species showing significant nuclear uptake with nuclear DNA being the primary target of binding. We have recently shown that similar charge neutral platinum(II) catecholates of 2-(phenylazo)pyridine (pap) are efficient photocytotoxic agents giving IC_{50} values of ~5 μM in visible light (400-700 nm) in HaCaT (human skin keratinocytes) and MCF-7 (human breast cancer) cells with low dark toxicity (IC_{50} >40 μM) and significant nuclear uptake.[13] The anticancer activity is due to glutathione (GSH)-triggered release of the catecholate ligand to generate an active pap-bound platinum(II) species as a DNA crosslinker. The released photoactive catecholate acts as a phototoxin. With a follow-up to this work we have successfully prepared a cis-diammineplatinum(II) complex of curcumin (Hcur) and this complex, named as Platicur, showed photoactivated curcumin release thus forming dual action DNA crosslinking and photochemotherapeutic agents.[14] Unlike the conventional platinum(II) drugs, $[Pt(cur)(NH_3)_2](NO_3)$ is a monocationic species with curcumin in its enolic form as a monoanionic β-diketonate ligand. Interestingly, the complex displays cytosolic localization in preference to the nuclear uptake. Utilizing the Pt-O(cur) bond dissociation on photo-activation, this complex exemplified a prodrug that leads to facile cellular delivery of curcumin (Hcur) which is an active ingredient of turmeric with important medicinal values.[15-19]

[a] *Department of Inorganic and Physical Chemistry, Indian Institute of Science, Bangalore 560012, India*
[b] *Department of Molecular Reproduction, Development and Genetics, Indian Institute of Science, Bangalore 560012, India.*
# Authors contributed equally to the manuscript.

† Electronic Supplementary Information (ESI) available: spectral and electrochemical plots, DNA binding, cleavage, cellular and DFT data (Scheme S1, Fig. S1 – S42, Table S1). See DOI: 10.1039/b000000x/

The present work stems from our interests to design platinum(II) complexes of monoanionic β-diketonate ligands like curcumin (Hcur) and acetylacetone (Hacac) derivatives having photoactive moieties (Hpy-acac, Han-acac) and study their photochemotherapeutic activity. Organometallic compounds have recently been found to be promising anticancer drug.[20] The choice of organometallic, a monoanionic C,N-donor azo ligand is to obtain charge neutral complexes while the presence of monoanionic O,O-donor β-diketonate ligands ensures slow release of the ligand to generate an active platinum(II) species that could possibly form covalent linkage to the cellular DNA. The cyclometallated platinum(II) moiety is expected to have a $\{Pt^{II}(C^{-},N)\}^{+}$ core which is stable in a cellular medium like the well known active platinum(II) species.[21-23] The objective of using curcumin (Hcur) and pyrenyl/anthracenyl appended acetylacetonates as β-diketonates is to achieve photo-induced and/or glutathione-triggered generation of two active species, viz. a cisplatin analogue as the cytotoxin and the released curcumin/acac derivatives as phototoxins. GSH as a non-protein thiol is the key regulator for various biological processes involving the platinum-based drugs.[24,25] An elevated level of GSH is found in most cancer cells (~15 mM) and it could act as a potent tumour target. Recent reports have shown that platinum(II) and half-sandwich organometallic (η^6-arene)ruthenium(II) complexes are highly cytotoxic because of the redox reactions of the metal-coordinated azo ligands and GSH.[13,26-30] As mentioned above, the GSH triggered release of the platinum(II) bound catecholate ligands is shown to enhance the efficacy of the complexes on targeting different cellular organelles.[13,31-33] Herein, we report platinum(II) complexes [Pt(L)(cur)] (**1**), [Pt(L)(py-acac)] (**2**) and [Pt(L)(an-acac)] (**3**), where HL is 4,4'-bis-dimethoxyazobenzene, Hcur is curcumin, Hpy-acac is pyrenylacetylacetone and Han-acac is anthracenylacetylacetone (Fig. 1). Complex [Pt(L)(acac)] (**4**) of acetylacetone (Hacac) was prepared and used as a control. The significant results of this work include photocytotoxicity of the complexes **1**-**3** in skin keratinocytes HaCaT cells giving IC_{50} values of 8-14 μM in visible light (400-700 nm, 10 J cm^{-2}), while being significantly less toxic in the dark (IC_{50}: ~60 μM).

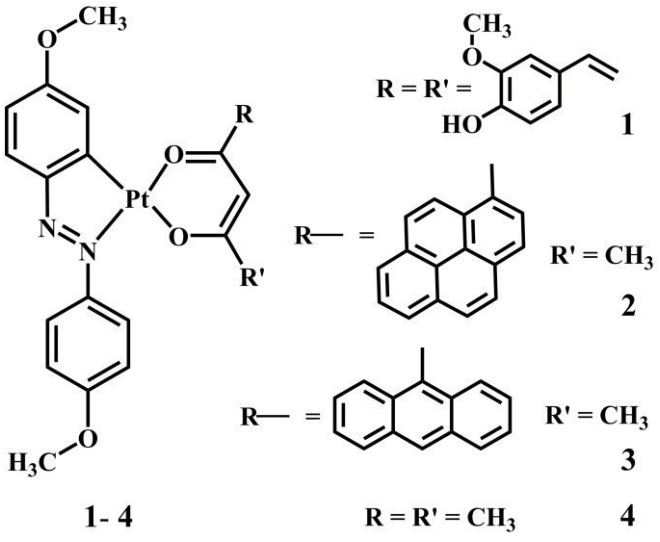

Fig. 1. Chemical structures of the complexes **1**-**4**.

Result and Discussion

View Article Online
DOI: 10.1039/C6DT02590K

Synthesis and characterization

Complexes **1**-**4** were synthesized in high yields (~80%) from a general reaction involving a precursor platinum(II) allyl dimeric complex with 4,4'-bis-dimethoxyazobenzene in chloroform to obtain an intermediate species of formulation $[Pt(L)(\mu\text{-}Cl)]_2$ (Scheme S1, ESI†). This dimeric species was subsequently reacted with the thallium salt of the β-diketonates (Hcur for **1**, Hpy-acac for **2**, Han-acac for **3** and Hacac for **4**) in dichloromethane to isolate the desired products. Melting point measurements of the complexes **1**-**4** showed their decomposition at 180, 188, 168 and 145 ºC respectively. The complexes were characterized from their analytical and spectroscopic data (Fig. 2, Fig. S1-S24, ESI†). Selected physicochemical data are given in Table 1. The ESI-MS spectra of **1**-**3** in methanol displayed a single peak (respective m/z = 804.18, 722.17 and 698.16) corresponding to the $[M+H]^+$ species (Fig. S1-S3, ESI†). The isotopic distribution pattern indicated the presence of platinum in the complexes and the unipositive charge of the fragments the complexes under applied voltages. The ^1H NMR spectral data were used to characterize the diamagnetic platinum(II) complexes (Fig. S4-S7, ESI†). The β-diketonate ligands showed characteristic singlet peak in the range of 5.50-6.20 ppm, which is assignable to the hydrogen atom of the γ-protons of the methylene groups. The aromatic hydrogen atom peaks of the curcumin, pyrenyl or anthracenyl moiety were in the range of 7.0−8.9 ppm, while the hydrogen atoms of the azo liand gave signals within 6−8 ppm. The protons corresponding to the methoxy groups of the azo ligand were within 3.8-4.1 ppm. The NMR peaks observed near 2.0 ppm were assigned to the protons of the methyl groups. The ^{13}C NMR spectra of the ligands and their metal complexes showed the presence of C=O (β-diketonate moiety) carbons, giving signals within 190-160 ppm (Fig. S8-S13 ESI†). The carbon atoms of complex **1** bearing the OH moiety appeared at 142 and 148 ppm. The characteristics γ-carbon peaks of the β-diketonate moiety for free ligands and in metal bound form showed signals within 110-90 ppm. The signals around 35-25 ppm were assignable to the methyl carbon atoms. The ^1H and ^{13}C NMR spectra of the complexes showed peaks similar to those observed for the free ligands. Some additional peaks in the aromatic region were observed in the spectra of the complexes, which are due to carbon atoms of the azo ligand. The IR spectra of the complexes showed disappearance of the signal of the O-H stretching frequency around 3400-3500 cm^{-1}, present in the free ligands, indicating the loss of hydrogen atom upon binding to the metal ion. Two intense peaks within 1600-1610 and 1590-1490 cm^{-1} are due to respective C=O (β-diketonate moiety) and conjugated C=C of acac derivatives stretching frequencies. The metal bound azo N=N of the 4,4'-dimethoxyazobenzene ligand showed sharp characteristic peaks near 1250 cm^{-1} (Fig. S14-S20, ESI†). The complexes gave molar conductance values of ~30 S m^2 M^{-1} in DMF at room temperature suggesting their non-electrolytic nature. Platinum azo complexes are well known for their redox properties.[34] The cyclic voltammograms of the complexes in DMF-0.1M TBAP (tetrabutylammonium perchlorate) showed two responses near –1.1 and –0.85 V vs. SCE (Fig. S21, S22, ESI†). The responses that are quasi-reversible or irreversible in nature are assignable to two-step azo reductions. The absorption spectra of the complexes were recorded in 10% DMSO-DPBS solutions (pH, 7.2) (Fig. 2a). Complexes **1**-**3** showed an intense absorption band near 400 nm with high ε values. Complex **4** displayed one weak absorption band near 412 nm. The complexes displayed a band at ~540 nm that arises from transitions involving the Pt(II) coordinated azo ligand. The low ε values for **4** indicates the important role of the photoactive β-diketonate moieties. The curcumin analogue **1** showed an emission band at 525 nm (λ_{ex} = 430 nm) in DMSO–water (3:1 v/v) at 25 °C with a quantum yield (Φ) value of 0.017 (Fig. 2b). The pyrenyl and anthracenyl complexes

also exhibited characteristic structured emissive bands at 440 and 435 nm (Φ of 0.058 and 0.045).[35] The free ligands mimicked the emission spectra of respective complexes (Φ within 0.020 to 0.067) (Table 1, Fig. S23, S24, ESI†). Significant reduction in the emission intensity and low Φ value make these complexes unsuitable for cellular imaging studies.

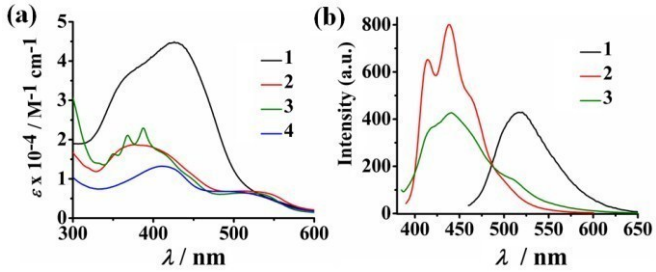

Fig. 2. (a) Absorption spectra of **1**-**4** in 10% DMSO-DPBS. (b) Emission spectra of **1**-**3** in aq. DMSO (1:3 v/v) (λ_{ex}: 430 nm, **1**; 370 nm, **2;** 365 nm, **3**).

Theoretical study

Computational studies were carried out using B3LYP/LanL2DZ level of theory with G09 suites of programs to gain insights into the photophysical properties of the complexes.[36-38] The initial coordinates for the complexes were directly taken from the reported crystal structure of **4** and then modified by adding fragments as per the requirement.[39] These coordinates were then utilized for obtaining energy-minimized structures of **1**-**3** using density functional theory (DFT) (Table S1, Fig. S25, ESI†). The frontier orbital diagrams shown in Fig. 3 reveal that the HOMO in **1**-**3** mainly resides on the platinum bound azo moiety having small contributions from the O,O-donor ligands. For **1**, the LUMO has significant contributions from both curcumin and the azo ligand (Fig. 3b). However, for **2** and **3**, the orbital contribution from LUMO is dominated by the platinum bonded azo moiety (Fig. S26, ESI†). Importantly, these orbitals are dissociative in nature indicating the possibility of the Pt–O bond cleavage.[40,41]

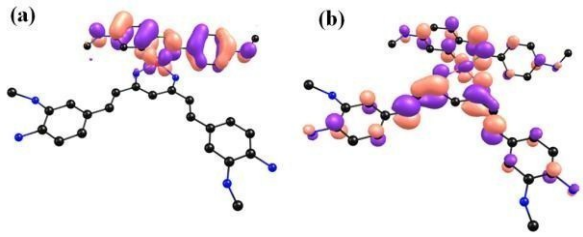

Fig 3. (a) Frontier molecular orbitals of complex **1** as obtained by DFT calculations using B3LYP/LanL2DZ level of theory: (a) HOMO and (b) LUMO. Colour codes: Pt, red; O, blue; N, green; C, black. Hydrogen atoms are omitted for clarity.

Solubility and stability

The complexes were moderately soluble in common organic solvents other than the hydrocarbons. They were stable in both solid and solution phases. The stability of the complexes was studied in the dark and in presence of cellular analytes by UV-visible, mass and NMR spectral measurements. The complexes (50 μM in 10% DMF-DPBS) showed slow degradation at 37 ºC as seen from the loss in intensity in the absorption bands in the visible region (Fig. S27, S28 ESI†). Curcumin was found to be more stable in the metal bound form in **1** under similar conditions. The time dependent ^{1}H NMR spectral study in deuterated dimethyl sulfoxide up to 24 h at 37 ºC showed that complexes are stable. Complex **1** and **2** were found to be more stable than **3** showing appearance of free ligand peaks on longer duration of the experiment (Fig. S29, S30 ESI†). Complexes **1**-**3** (25 μM) in DMSO-DPBS buffer (3:2 v/v) were treated with increasing equivalents of glutathione (GSH, 50-650 μM) and emission spectra recorded are shown in Fig. 4 (Fig. S31, ESI†). A GSH concentration dependent enhancement in the emission intensity was observed suggesting possible cleavage of the Pt-O bonds, thereby releasing the β-diketonate ligands.[42,43] The emission intensity reached a saturation indicating complete release of the ligands. The samples when diluted with methanol and subjected to mass spectrometry showed the presence of free ligands with m/z value of 369.13 for HCur in **1**, 287.11 for Hpy-acac in **2** and 263.10 for Han-acac in **3** (Fig. S32-S34, ESI†). An additional peak in the mass spectra of the GSH treated complexes was observed at m/z of 759.23 (Fig. S32, ESI†). This was assigned to a GSH bound {Pt(L)} species. Time-dependent ^{1}H NMR studies also corroborated the leaching out of β-diketonate ligands from the platinum(II) complexes. The peak observed at 6.1 ppm is assignable to the γ-H proton of the free ligand. Interestingly, formation of any GSSG was not observed in the mass and ^{1}H NMR spectra postulating that GSH is not undergoing any redox reaction but merely substituting the O,O-donor ligand (Fig. S35, ESI†). This is different from what is reported on the platinum(II) catecholates.[13] Thus, we conclude that the C,N-donor azo ligand behaves differently than its N,N-azo analogue. This is also supported from the absence of any GSH accessible redox peak in the complexes near –0.34 V which was previously observed for the 2-(phenylazo)pyridine (pap) platinum(II) catecholates.

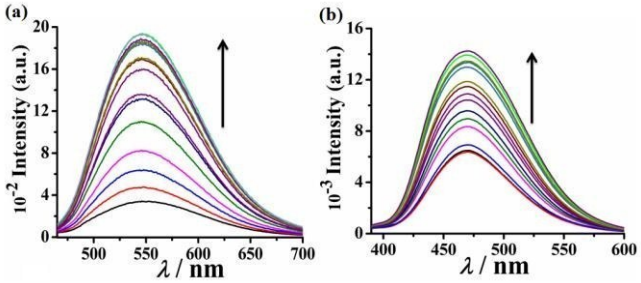

Fig 4. Change in the emission spectra of the complexes **1** (a) and **2** (b) on addition of GSH (50-650 μM) in DMSO-DPBS buffer (3:2 v/v).

DNA binding and cleavage

Platinum drugs viz. cisplatin and its analogues are known to target nuclear DNA. Moreover, the complexes under present investigation showed release of the active Pt(II) species and the O,O-donor ligands in presence of GSH. The resulting species are capable of interacting with DNA. We thus explored the calf thymus (ct) DNA binding properties from absorption titrations and viscosity measurements. Complexes **1** and **4** did not show any apparent

decrease in the absorption intensity upon addition of ct-DNA in absence of any intercalating moiety giving moderate DNA binding constant (K_b) values of 1.5(±0.3) x 10^4 for **1** and 1.2 (±0.4) x 10^3 M^{-1} for **4** (Fig. 5a, Table 1, Fig. S36, ESI†). Complexes **2** and **3** and ligands Hpy-acac and Han-acac having planar pyrenyl and anthracenyl group showed significant hypochromicity when treated with ct-DNA.[44-46] The K_b values of these compounds having planar moiety are ~5.0 x 10^5 M^{-1} indicating their DNA groove and/or intercalative binding propensity. In contrast, the curcumin and acac complexes showed only surface binding to DNA.

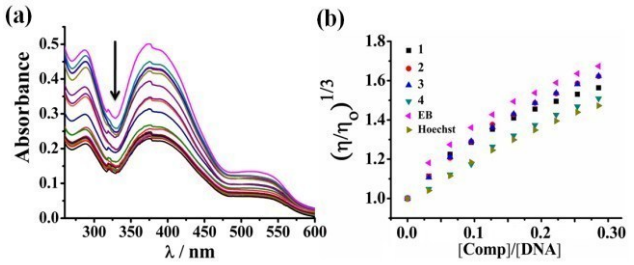

Fig. 5. (a) Spectral changes on addition of ct-DNA to complex **2** in DMF-Tris-HCl buffer (pH = 7.2). (b) Effect of addition of **1-4**, ethidium bromide (EB) and Hoechst 33258 on ct-DNA (170 μM) relative viscosity at 37.0(±0.1) ºC in 5 mM PBS buffer (pH = 6.8).

The DNA binding interactions were additionally examined by viscometric titrations.[47] The DNA contour length is known to get affected in different ways in the presence of intercalating molecules, groove and surface binders. This effect is analysed from the observed increase in the relative specific viscosity of the ct-DNA. Intercalation results in an increase in the viscosity of DNA as compared to the groove or surface interactions. The viscosity plots for **2** and **3** are similar to that of ethidium bromide (EB) indicating their intercalative mode of binding to ct-DNA (Fig. 5b). The curcumin and acac complexes **1** and **4** showed only minor changes in the relative viscosity similar to that of the DNA minor groove binder Hoechst 33258 dye. The DNA binding data suggest the pyrenyl and anthracenyl complexes as DNA intercalators, while their curcumin analogue is a DNA surface binder.

The DNA photocleavage study was carried out with complexes **1-3** and the free ligands (15 µM) using supercoiled (SC) pUC19 DNA (30 µM, 2686 bp) in Tris-HCl buffer solution (pH = 7.2) to explore the effect of the photoactive diketonate ligands on the DNA cleavage activity of the complexes. Irradiation was done with a laser of 457 nm (50 mW power). The DNA cleavage potential is estimated from the percentage of nicked-circular (NC) DNA formed from the agarose gel electrophoresis assay. Complexes **1-3** exhibited efficient photocleavage of SC DNA giving 50-75% of NC DNA (Fig. 6, Fig. S37a, ESI†). The acac analogue did not show any photocleavage of DNA. The photocleavage activity of **1-3** resulted from the activation of the charge transfer band near 400 nm. The ligands alone showed reduced DNA photocleavage activity under similar experimental conditions thus indicating the importance of the platinum(II) centre for production of the reactive oxygen species (ROS).[48] All the complexes and ligands were inactive in the dark. Complexes **1-3** (20 µM) when incubated with SC DNA in presence of an oxidizing agent (H_2O_2, 5 mM) or a reducing agent (GSH, 5 mM) in dark for 1h showed SC DNA as the predominant form indicating no apparent chemical nuclease activity of the complexes (Fig. S37b, ESI†).

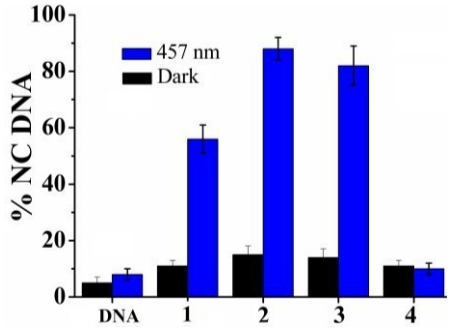

Fig. 6. Bar diagram showing photo-induced pUC19 DNA (0.2 µg, 30 µM b.p.) cleavage by **1-4** (15 µM) in blue light of 457 nm (blue bars) and in the dark (black bars) [NC, nicked circular].

Cellular study

The antiproliferative properties of the complexes were investigated in immortalised human skin keratinocytes (HaCaT) cell lines using 3-(4,5-dimethylthiazole-2-yl)-2,5-diphenyl tetrazolium bromide (MTT) assay (Fig. 7, Fig. S38, ESI†).[49] HaCaT cells were chosen as the therapeutic action of curcumin as an active ingredient of turmeric is well documented for skin related disorders. The cells were treated with the complexes or the ligands for 4 h. The half maximal inhibitory concentrations (IC_{50}) in both dark and light are listed in Table 2. The light exposure was done using visible light of 400-700 nm (Luzchem photoreactor, 10 J cm^{-2}). Complexes **1-3** resulted significant photocytotoxic effect in visible light giving IC_{50} values in the range of 8-14 µM. The dark toxicity ranged within IC_{50} values of 45 and 61 µM. The intracellular interaction of these complexes with GSH could facilitate release of active platinum(II) species as transcription inhibitor thus enabling the complexes to show minor dark toxicity.[50,51] Ligands Py-acac/An-acac showed higher IC_{50} values compared to the complexes in light. The ligands alone are thus not responsible for the observed cytotoxicity suggesting important contribution of the metal.The photo-inactive acac complex **4** showed no apparent photocytotoxic effect.

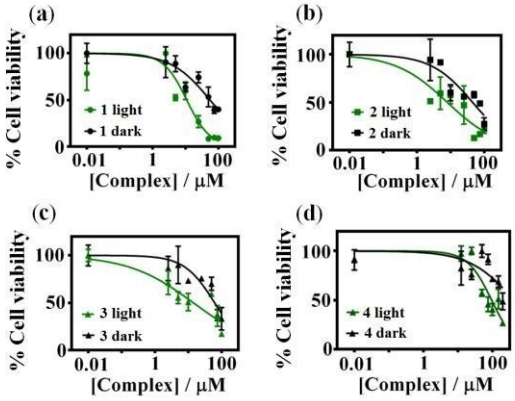

Fig. 7. Cell viability plots (a) – (d) showing cytotoxicity of the respective complex **1-4** in HaCaT cells [black symbols in the dark; green symbols in visible light (400-700 nm, 10 J cm^{-2})].

DCFDA (2',7'-dichlorofluorescein diacetate) assay was performed using flow cytometry to detect any ROS formation. The non-fluorescent DCFDA dye on enzymatic reaction forms H_2DCF which upon oxidation by ROS generates fluorescent DCF with an emission maximum at 528 nm. The DCF intensity directly correlates to the amount of ROS. Complex **1** (20 μM) showed pronounced generation of ROS on irradiation with visible light (400-700 nm) as indicated by an increase in DCF mean intensity shown in Fig. 8. The complex also showed some ROS production in dark possibly from the reaction of the platinum(II) species with GSH.

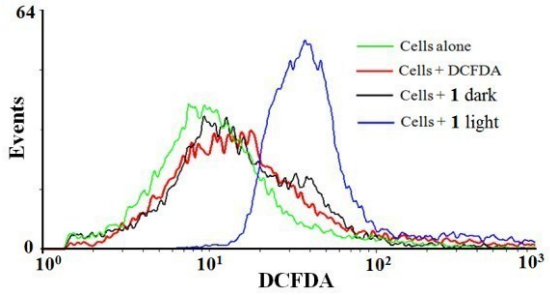

Fig. 8. Shift in band positions of complex **1** in HaCaT cells in light (400-700 nm, 10 J cm^{-2}) with colour code: green, cells only; red, cells + DCFDA; black, cells + DCFDA + complex in dark; blue, cells + DCFDA + complex exposed to visible light (400-700 nm).

The changes in chromatin organization after light irradiation in HaCaT cells were determined microscopically after treatment with the complexes **1**-**3** by acridine orange and ethidium bromide (AO/EB) dual staining method. The experiment is based on the discrimination of live cells from the dead ones on the basis of membrane integrity. AO stains the DNA of live cells and shows green fluorescence. EB is excluded from the cells having intact plasma membrane and stains the DNA of dead cells showings orange fluorescence. HaCaT cells treated with **1**-**3** (20 μM) for 4 h and kept in the dark showed green fluorescence corresponding to the emission of AO. However, when the experiment was performed after visible light exposure, the intensity of red emission increased significantly indicating photo-induced cell death (Fig. 9, Fig. S39, ESI†).

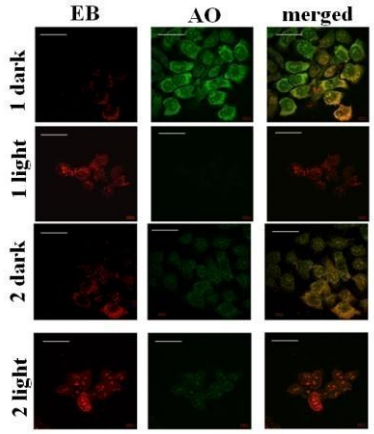

Fig. 9. Ethidium bromide (EB)/acridine orange (AO) dual staining images of complexes **1** and **2** in light and in the dark as shown in the figure. Scale bar = 10 μm.

Annexin V-FITC/PI assay was done to study any cellular apoptosis on light exposure using HaCaT cells treated with the complexes. Propidium iodide (PI) emits in the red region, while the annexin V-FITC dye shows green fluorescence. This staining allowed us to quantify the apoptotic cell. From the dot plots shown in Fig. 10 (Fig. S40-S42, ESI†), where lower left is for live cells, lower right is for early apoptotic cells, upper right is for late apoptotic cells and upper left is for dead cells, we can infer that the percentage cell population in the lower right quadrant increased to ~22% (for **1**) and ~5% for **4** when HaCaT cells were treated with the complexes **1**-**4** and exposed to light (400-700 nm) than when kept in the dark. This indicates light induced early apoptotic cell death promoted in presence of the complexes. Complex **4** did not show any significant apoptosis in the dark or in light.

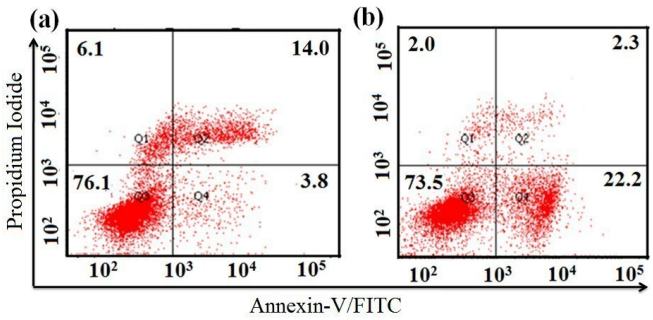

Fig. 10. Annexin V-FITC/PI assay using FACS in HaCaT cells with 4 h incubation of complex **1** (20 μM) in the dark (a) and in light (b) (400-700 nm, 1h). The % cell population is shown in respective quadrants [lower left: live cells, lower right: early apoptotic cells, upper right: late apoptotic cells, upper left, dead cells].

Platinum uptake

The cellular uptake was evaluated in terms of platinum content of the cell and expressed as ng platinum per 10^6 cells. HaCaT cells were incubated for 4h in the dark with the complexes **1**-**4** (20 μM) and the platinum content of the cell lysates dissolved in 2% HNO_3 was estimated using ICP-MS method along with the untreated cells and standard platinum solutions. The cellular uptake values (ng Pt/ 10^6 cells) of **1**-**4** are 2510, 110, 120, and 60, respectively (Table 2). Complex **4** showed poor lower cellular uptake than the complexes **1**-**3** due to lipophilicity of the complexes. The presence of curcumin in metal-bound form could be responsible for the significantly higher platinum uptake of complex **1**.

Conclusions

The C,N-donor azo organometallic platinum(II) complexes of β-diketonates **1**-**3** are remarkably PDT active giving IC_{50} values of ~10 μM in visible light (400-700 nm) while being less toxic in the dark (IC_{50}: ~60 μM). The complexes could be photo-activated using their intense absorption band near 400 nm. The complexes are susceptible to Pt-O bond cleavage on photo-activation. The photoactive β-diketonate base acts as a phototoxin. Complexes **2** and **3** having planar extended aromatic pyrenyl and anthracenyl

pendant moieties are excellent DNA binders showing intercalative binding properties. The complexes showed apoptotic cell death via generation of light mediated ROS. The DNA photocleavage studies reveal the nature of ROS as the hydroxyl radicals. The present complexes exemplify organometallic platinum(II) complexes as anticancer agents suitable for selective delivery of photoactive β-diketonato bases that includes curcumin, an active ingredient of turmeric.

Experimental Section

Materials

The chemicals were procured from commercial sources and used as received (s. d. Fine Chemicals, India; Aldrich, USA). Potassium tetrachloroplatinate was obtained from Arora Matthey, India. Solvents were purified by known procedures.[52] Supercoiled (SC) pUC19 DNA (cesium chloride purified) was from Bangalore Genie (India). Tris-(hydroxymethyl)aminomethane-HCl (Tris-HCl) buffer solution was prepared using deionized and sonicated triple distilled water. Calf thymus (ct) DNA, agarose (molecular biology grade), ethidium bromide (EB), 3-(4,5-dimethylthiazol-2-yl)-2,5-diphenyltetrazolium bromide (MTT) and 2',7'-dichlorofluorescein diacetate (H_2DCFDA) were purchased from Sigma Aldrich (USA). Tetrabutylammonium perchlorate (TBAP) was prepared by reacting tetrabutylammonium bromide with perchloric acid (Caution! TBAP being a perchlorate salt should be handled with care). The ligands, viz., 4,4-bismethoxyazobenzene, Hpy-acac and Han-acac were prepared following literature reports.[53,54] Complex $[(\eta^3\text{-}C_4H_7)Pt(\mu\text{-}Cl)]_2$ and complex **4** were prepared by a modified literature procedure.[39] For the precursor complex having monoanionic bidentate L, $[(\eta^3\text{-}C_4H_7)Pt(\mu\text{-}Cl)]_2$ (143 mg, 0.25 mmol) and HL (121 mg, 0.50 mmol) in chloroform (25 ml) were mixed and refluxed for 30 h, cooled and filtered. A red solid thus obtained was dried in vacuum. [Tl(acac)] was prepared in quantitative yield by reacting acetylacetone (0.11 mol) in 50 ml petroleum ether with thallium(I) ethoxide (0.10 mol) and the mixture was stirred for ~5 min, chilled and filtered.[55] The thallium salts of Hcur, Hpy-acac and Han-acac were prepared in a similar way.

Measurements

The elemental analysis was performed using a Thermo Finnigan FLASH EA 1112 CHNS analyzer. The IR and UV-visible spectra were recorded on Perkin Elmer Lambda 35 and Perkin Elmer spectrum one 55 spectrometer, respectively. Cyclic voltammograms were recorded on an EG&G PAR model 253 VersaStat potentiostat/galvanostat with electrochemical analysis software 270 using a three electrode setup consisting of a glassy carbon working, platinum wire auxiliary and a saturated calomel reference electrode (SCE) in DMF and using TBAP (0.1 M) as a supporting electrolyte. For molar conductivity measurements, a Control Dynamics (India) conductivity meter was used. Electrospray ionization (ESI) mass spectral measurements were made using Agilent 6538 Ultra High Definition QTOF (LC-HRMS) mass spectrometer. The NMR spectra were recorded using Bruker Avance 400 (400 MHz) NMR spectrometer. The platinum content was obtained by ICP-MS method using Thermo X series II instrument.

Synthesis

Complexes **1-4** were prepared by following a general procedure. The precursor complex $[(L)Pt(\mu\text{-}Cl)]_2$ (226 mg, 0.24 mmol) was treated with [Tl(β-diketonate)] (274 mg, 0.48 mmol for **1**; 235 mg, 0.48 mmol for **2**; 223 mg, 0.48 mmol for **3** and 146 mg, 0.48 mmol for **4**) in dichloromethane (15 ml) and stirred for 6 h at 30 °C. The reaction mixture was filtered off and the solution was evaporated under reduced pressure in a rotavac. The solid was isolated from methanol solution on slow evaporation and dried under vacuum. The product was isolated as a solid (red for **1**-**3** and brown for **4**).

Complex **1**: yield 84% (163 mg). Anal. Calcd for $C_{35}H_{32}N_2O_8Pt$ (Mol wt = 803.71 g mol^{-1}): C, 52.30; H, 4.01; N, 3.49. Found: C, 52.13; H, 4.06; N, 3.67. ESI-MS in MeOH: m/z observed, 804.1826; calculated, 804.1885 $[M+H]^+$. IR data/cm^{-1}: 3384 w, 3068w, 1605, 1585 s, 1510vs, 1433 w, 1315 m, 1245 vs, 1166 m, 1022 s, 980 m, 834 m, 786 s, 598 w, 532 m (vs, very strong; s, strong; m, medium; w, weak). ^{1}H NMR (400 MHz, DMSO-d_6) [δ (ppm)]: 7.90 (d, J = 8.9 Hz, 2H), 7.76 (d, J = 9.2 Hz, 2H), 7.58-7.41 (m, 6H), 7.31 (s, 1H), 7.22-7.03 (m, 5H), 6.92 (s, 1H), 5.94 (s, 1H), 4.03(s, 6H), 3.87(s, 3H), 3.831 (s, 3H). ^{13}C NMR (100 MHz, DMSO-d6): δ 178.10, 176.26, 165.03, 161.12, 158.51, 149.97, 148.28, 145.10, 141.37, 140.29, 133.83, 130.77, 127.79, 123.47, 119.92, 116.82, 114.39, 113.65, 111.80, 97.08, 56.75, 49.51.

Complex **2**: yield 81% (141 mg). Anal. Calcd for $C_{34}H_{27}N_2O_8Pt$ (Mol wt = 721.68 g mol^{-1}): C, 56.51; H, 3.77; N, 3.88. Found: C, 56.83; H, 3.86; N, 3.69. ESI-MS in MeOH: m/z observed, 722.1741; calculated, 722.1619 $[M+H]^+$. IR data/cm^{-1}: 3384 w, 3068w, 1602, 1587 s, 1509 vs, 1433 w, 1315 m, 1245 vs, 1166 m, 1022 s, 980 m, 834 m, 786 s, 598 w 532 m. ^{1}H NMR (400 MHz, $CDCl_3$): δ (ppm) 8.76 (d, J = 7.2 Hz, 2H), 8.36-7.88 (m, 9H), 7.82 (d, J = 8.4 Hz, 2H), 7.62 (d, J = 8.0 Hz, 2H), 7.51 (d, J = 7.9 Hz, 2H), 6.20 (s, 1H), 3.99 (s, 3H), 3.50 (s, 3H), 2.27 (s, 3H). ^{13}C NMR (100 MHz, $CDCl_3$): δ 187.42, 176.03, 165.41, 142.18, 132.49, 131.90, 130.25, 129.48, 128.98, 127.02, 126.80, 125.72, 124.83, 113.04, 42.82, 24.37.

Complex **3**: yield 79% (134 mg); Anal. Calcd for $C_{32}H_{26}N_2O_4Pt$ (Mol wt = 697.45 g mol^{-1}): C, 55.09; H, 3.76; N, 4.02. Found: C, 54.82; H, 3.84; N, 4.16. ESI-MS in MeOH: m/z observed, 698.1620: calculated, 698.1619 $[M+H]^+$. IR data/cm^{-1}: 3054 w, 1598 s, 1501 vs, 1430 w, 1383 m, 1315 m, 1246 vs, 1154 m, 1110 m, 1022 s, 946 w, 834 s, 792 m, 730 s, 668 m, 598 m, 526 s. ^{1}H NMR (400 MHz, $CDCl_3$): δ (ppm) 8.56 (s, 1H), 8.03 (d J = 6.8 Hz, 4H), 7.91 (d, J = 7.2 Hz, 2H), 7.88 (d, J = 8.3 Hz, 2H), 7.52 (d, J = 3.4 Hz, 2H), 7.01 (d, J = 8.2 Hz, 4H), 6.97 (s, 1H), 5.97 (s, 1H), 4.01 (s, 3H), 3.88 (s, 3H), 2.20 (s, 3H). ^{13}C NMR (100 MHz, $CDCl_3$): δ 187.12, 180.11, 163.45, 142.31, 131.52, 129.43, 128.81, 127.10, 126.64, 125.73, 113.75, 105.76, 58.19, 26.38.

Complex **4**: yield 82% (103 mg); Anal. Calcd for $C_{19}H_{20}N_2O_4Pt$ (Mol wt = 535.45 g mol^{-1}): C, 42.62; H, 3.76; N, 5.23. Found: C, 42.32; H, 3.84; N, 4.86. IR data/cm^{-1}: 3064 w, 1612 s, 1502 vs, 1453 m, 1321 w, 1251 vs, 1168 m, 1126 m, 1022 s, 960 w, 828 s, 764 w, 612 w, 528 s. ^{1}H NMR ($CDCl_3$): δ (ppm) 7.91 (d, J = 9.1 Hz, 2H), 7.10 (d, J = 8.6 Hz, 2H), 6.97 (d, J = 2.8 Hz, 1H), 6.76 (d, J = 9.1 Hz, 1H), 6.74 (s, 1H), 5.51 (s, 1H), 3.94 (s, 3H), 3.88 (s, 3H), 2.07 (s, 3H), 1.98 (s, 3H).

Cellular experiments

MTT assay: The photocytotoxicity of the complexes was studied using MTT assay. Approximately, 8000 cells of human skin keratinocyte (HaCaT) cells were plated separately in 96 wells culture plate in high glucose Dulbecco's Modified Eagle Medium (DMEM) containing 10% FBS. After 24 h of incubation at 37 °C in a CO_2 incubator, various concentrations of the complexes dissolved in 1% DMSO were added to the cells and incubation was continued for 4 h in the dark. The media was subsequently replaced with DPBS and irradiated with a broad band visible light (400-700 nm, 10 *J* cm^{-2}) using a Luzchem Photoreactor (Model LZC-1, Ontario, Canada) fitted with Sylvania make 8 fluorescent white tubes. After photo-exposure, DPBS was removed and replaced with DMEM-FBS and incubation was continued for a further period of 20 h in the dark. After the incubation period, 5 mg ml^{-1} of MTT (20 µL) was added to each well and incubated for an additional 3 h. The culture medium was finally discarded and 200 µL of DMSO was added to dissolve the formazan crystals and its absorbance at 540 nm was measured using a Molecular Devices Spectra Max M5 plate reader (100-240 V, 3.5 A, 50-60 Hz). Cytotoxicitiy of the complex was measured as the percentage ratio of the absorbance of the treated cells to the untreated controls. The IC_{50} values were determined by nonlinear regression analysis (GraphPad Prism 5).

DCFDA assay: 2',7'-Dichlorofluorescein diacetate was used to detect the generation of cellular ROS. Cell permeable DCFDA on oxidation by cellular ROS generates a fluorescent DCF having an emission maximum at 528 nm. The percentage of cell population generating ROS was determined by flow cytometry analysis. HaCaT cells were incubated with **1** (20 µM) for 4 h followed by photo-irradiation (400-700 nm) for 1 h in DPBS. These cells, after irradiation, were harvested by trypsinization and a single cell suspension of $1x10^6$ cells ml^{-1} was made. The cells were then treated with 1µM DCFDA solution in DMSO in dark for 15 min at room temperature. The distribution of DCFDA stained HaCaT cells was determined by flow cytometry in the FL-1 channel.

EB/AO assay: The changes in chromatin organization after light irradiation in HaCaT cells were determined microscopically after treatment with the complexes **1**-**3** by dual staining method using acridine orange (AO) and ethidium bromide (EB). Briefly, about 2 x 10^4 cells were allowed to adhere overnight on a cover slip placed in each well of 12-well plate. The cells were treated with the complexes (20 µM) for 4 h in the dark, followed by irradiation with visible light of 400-700 nm (10 *J* cm^{-2}). Dark controls were also used. The cells were allowed to recover for 1 h, washed thrice with DPBS, stained with an AO/EB mixture (1:1, 10 µM) for 15 min, and observed with a confocal laser scanning microscope (Zeiss LSM 510 apochromat).

Annexin V-FITC/PI assay: HaCaT cells (3 x 10^5) were plated in 6 well plates and grown for 24 h. Cells were incubated with the complexes **1**-**4** and cisplatin (20 µM) for 4 h. The medium was removed and the samples were irradiated for 1 h (400-700 nm, 10 *J* cm^{-2}) in DPBS. After treatment, cells were allowed to grow for 10 h, washed twice in DPBS and trypsinized. These cells were re-suspended in 400 µL of 1X binding buffer. Later 1 µL of annexin V-FITC and 0.5 µL of PI were added to each cell suspension. These were incubated at room temperature for 10 min and protected from light. The fluorescence of the cells was determined immediately with a flow cytometer. Cells in the early apoptosis showed high annexin V-FITC staining, while the ones in late apoptotic stage showed high PI and annexin V-FITC staining. Live cells showed no staining by either PI or annexin V-FITC and dead cells were stained only by PI.

DNA binding and cleavage

The DNA binding experiments were done using complexes **1**-**4** and calf thymus (ct)-DNA by UV-visible absorption spectroscopy and the intrinsic equilibrium binding constant (K_b) values were obtained by McGhee-von Hippel (MvH) method using the expression of Bard and co-workers (vide ESI† for details).[42] The viscometric titration experiments were performed to determine the relative specific viscosity of ct-DNA solution (130 µM) in 5 mM phosphate buffer in the presence of the complexes **1**-**4**. Relative specific viscosity of DNA, $(\eta/\eta_0)^{1/3}$, was plotted against [complex]/[DNA], where η and η_0 are the viscosity of DNA in the presence and absence of the complexes. The cleavage of supercoiled (SC) pUC19 DNA (0.2 µg, 30 µM, 2686 base-pairs) was determined by agarose gel electrophoresis using the complexes in 50 mM Tris–HCl buffer (pH 7.2) and 50 mM NaCl containing 10% DMF. The photo-induced DNA cleavage reactions were done using Ar-Kr mixed gas ion monochromatic CW laser (Spectra Physics, power = 50 mW) of 457 nm based on the absorption spectral band at ~428 nm of the complex and curcumin. The laser power was measured using Spectra Physics CW Laser Power Meter (Model 407A)). The observed error in measuring the band intensities was ~5%. The DNA photocleavage experiments were carried out with the complexes and the free ligands (15 µM) using supercoiled (SC) pUC19 DNA (30 µM, 2686 bp) in Tris-HCl buffer solution (pH = 7.2). The DNA cleavage potential was expressed as % of nicked-circular (NC) DNA as determined from the agarose gel electrophoresis assay. The chemical nuclease activity measurements were done in presence of an oxidizing agent (H_2O_2, 5 mM) or a reducing agent (GSH, 5 mM) in the dark for 1h.

Experiment on cellular uptake of platinum

To quantify the total platinum uptake, 3 x 10^5 HaCaT cells were plated in two 6 well plates. Cells were allowed to grow for 24 h and later treated with different platinum complexes (**1**-**4**) for 8 h. After the incubation period in both the set of 6 well plates the medium was aspired and all the wells were washed with PBS.

Later on one of the set was treated with 0.5 ml of hot (~90 °C) concentrated nitric acid for 2 h while its similar treatment counterpart was trypsinized and live cells were counted by using trypan blue method. Nitric acid treated samples were analyzed by ICP-MS to determine the total platinum content per well. In this assay medium alone was taken as a blank and the amount of platinum per cell was calculated by subtracting the average amount of platinum found in the blank wells from the average amount of platinum found in the cell containing wells and normalizing to the average number of cells per well.

Acknowledgements

We thank the Department of Science and Technology, Government of India, for financial support (SR/S5/MBD-02/2015, EMR/2015/000742) and the Alexander von Humboldt Foundation for donation of an electrochemical system. A.R.C. thanks the DST for J.C. Bose fellowship. P.K. acknowledges financial support from DBT-IISc partnership program. K.M. and A.S. thank respective funding agency for B.M.S. and UGC Kothari research fellowships. We thank Dr. Ramananda Chakrabarti, Centre of Earth Sciences CEaS, IISc, for the ICP-MS facility.

Notes and references

[a]Department of Inorganic and Physical Chemistry, Indian Institute of Science, Bangalore 560012, India.
E-mail: arc@ipc.iisc.ernet.in; Tel: +91-80-22932533
[b]Department of Molecular Reproduction, Development and Genetics, Indian Institute of Science, Bangalore 560012, India. E-mail: paturu@mrdg.iisc.ernet.in; Tel: +91-80-22933259

†Electronic Supplementary Information (ESI) available; spectral and electrochemical plots, DNA binding, cleavage, cellular and DFT optimization data (Scheme S1, Fig. S1–S31, Table S1). See DOI: 10.1039/b000000x/

References

1. (a) T. C. Johnstone, G. Y. Park and S. J. Lippard, *Anticancer Res.*, 2014, **34**, 471-476. (b) T. C. Johnstone, K. Suntharalingam and S. J. Lippard, *Chem. Rev.*, 2016, doi:10.1021/acs.chemrev.5b00597. (c) J. J. Wilson and S. J. Lippard, *Chem. Rev*., 2014, **114**, 4470-4495.
2. (a) R. K. Pathak, S. Marrache, J. H. Choi, T. B. Berding and S. Dhar, *Angew. Chem. Int. Ed.*, 2014, **53**, 1963-1967. (b) S. Marrache, R. K. Pathak and S. Dhar, *Proc. Natl. Acad. Sci. U.S.A.*, 2014, **111**, 10444-10449. (c) S. Dhar and S. J. Lippard, *Proc. Natl. Acad. Sci. U.S.A.*, 2009, **106**, 22199-22204.
3. X. Wang, X. Wang and Z. Guo, *Acc. Chem. Res.*, 2015, **48**, 2622-2631.
4. H. Cui, R. Goddard, K.-R. Pörschke, A. Hamacher and M. U. Kassack, *Inorg. Chem*., 2014, **53**, 3371-3384.
5. G. Sava, G. Jaouen, E. A. Hillard and A. Bergamob, *Dalton Trans*., 2012, **41**, 8226-8234.
6. L. Liu, Q. Ye, M. Lu, Y.-C. Lo, Y.-H. Hsu, M.-C. Wei, Y.-H. Chen, S.-C. Lo, S.-J. Wang, D. J. Bain and C. A. Ho, *Sci. Rep.*, 2015, **5**, 10881.
7. M. Patra, T. C. Johnstone, K. Suntharalingam and S. J. Lippard, *Angew. Chem. Int. Ed.*, 2016, **55**, 2550-2554.
8. (a) P. Štarha, I. Popa and Z. Trávníček, *Molecules*, 2014, **19**, 3832-3847. (b) R. Kitagawa, N. Katsumata, T. Shibata, T. Kamura, T. Kasamatsu, T. Nakanishi, S. Nishimura, K. Ushijima, M. Takano, T. Satoh and H. Yoshikawa, *J Clin Oncol.*, 2015, **33**, 2129-2135. (c). W. Liu, J. Su, J. Jiang, X. Li, Q. Ye, H. Zhou, J. Chen and Y. Li, *Sci. Rep.*, 2013, **3**, 2464.
9. (a) A. Naik, R. Rubbiani, G. Gasser and B. Spingler, *Angew. Chem. Int. Ed.*, 2014, **53**, 6938-6941. (b) C. Mari, V. Pierroz, A. Leonidova, S. Ferrari and G. Gasser, *Eur. J. Inorg. Chem.*, 2015, 3879-3891. (c) A. Frei, R. Rubbiani, S. Tubafard, O. Blacque, P. Anstaett, A. Felgentrager, T. Maisch, L. Spiccia, and G. Gasser, *J. Med. Chem.*, 2014, **57**, 7280-7292.
10. (a) E. Shaili, *Sci. Prog.*, 2014, **97**, 20-40. (b) T. J. Dougherty, C. J. Gomer, B. W. Henderson, G. Jori, D. Kessel, M. Korbelik, J. Moan and Q. Peng, *J. Natl. Cancer Inst.*, 1998, **90**, 889-905.
11. J. J. Wilson and S. J. Lippard, *J. Med. Chem*., 2012, **55**, 5326-5336.
12. (a) A. Muscella, N. Calabriso, F. P. Fanizzi, S. A. De Pascali, L. Urso, A. Ciccarese, D. Migoni and S. Marsigliante, *Br. J. Pharmacol.*, 2008, **153**, 34-49. (b) A. Muscella, N. Calabriso, C. Vetrugno, L. Urso, F. P. Fanizzi, S. A. De Pascali and S. Marsigliante, *Br. J. Pharmacol*., 2010, **160**, 1362-1377.
13. K. Mitra, S. Patil, P. Kondaiah, and A. R. Chakravarty, *Inorg. Chem*., 2015, **54**, 253-264.
14. K. Mitra, S. Gautam, P. Kondaiah, and A. R. Chakravarty, *Angew. Chem. Int. Ed*., 2015, **54**, 13989-13993.
15. (a) S. Banerjee and A. R. Chakravarty, *Acc. Chem. Res*., 2015, **48**, 2075-2083. (b) M. Pröhla, U. S. Schuberta, W. Weigandb and M. Gottschaldta, *Coord. Chem. Rev.*, 2016, **307,** 32-41.
16. (a) S. Prasad, A. K. Tyagi and B. B. Aggarwal, *Cancer Res. Treat.*, 2014, **46**, 2-18. (b) S. Wanninger, V. Lorenz, A. Subhan and F. T. Edelmann, *Chem. Soc. Rev.*, 2015, **44**, 4986-5002.
17. (a) A. K. Renfrew, N. S. Bryce and T. W. Hambley, *Chem. Eur. J*., 2015, **21**, 15224-15234. (b) A. K. Renfrew, N. S. Bryce and T. W. Hambley, *Chem. Sci*., 2013, **4**, 3731-3739.
18. (a) F. S. Mackay, J. A. Woods, P. Heringová, J. Kasparková, A. M. Pizarro, S. A. Moggach, S. Parsons, V. Brabec and P. J. Sadler, *Proc. Natl. Acad. Sci. U.S.A.*, 2007, **104,** 20743-20748. (b) J. S. Butler, J. A. Woods, N. J. Farrer, M. E. Newton and P. J. Sadler, *J. Am. Chem. Soc*., 2012, **134**, 16508-16511. (c) I. Romero-Canelón and P. J. Sadler, *Inorg. Chem.*, 2013, **52**, 12276-12291.
19. (a) K. L. Ciesienski, L. M. Hyman, D. T. Yang, K. L. Haas, M. G. Dickens, R. J. Holbrook and K. J. Franz, *Eur. J. Inorg. Chem.*, 2010, 2224-2228. (b) A. M. Pizarro, R. J. McQuitty, F. S. Mackay, Y. Zhao, J. A. Woods and P. J. Sadler, *ChemMedChem.*, 2014, **9**, 1169-1175. (c) Y. Zhao, N. J. Farrer, H. Li, J. S. Butler, R. J. McQuitty, A. Habtemariam, F. Wang, P. J. Sadler, *Angew. Chem. Int. Ed.*, 2013, **52**,

13633-13637. (d) M. Ethirajan, Y. Chen, P. Joshi and R. K. Pandey, *Chem. Soc. Rev.*, 2011, **40**, 340-362.
20. (a) A. Leonidova, C. Mari, C. Aebersold and G. Gasser, *Organometallics*, 2016, **5**, 851-854. (b) G. Gasser, I. Ott and N. Metzler-Nolte, *J. Med. Chem*., 2011, **54**, 3-25. (c) G. Gasser and N. Metzler-Nolte, *Curr. Op. Chem. Biol.*, 2012, **16,** 84-91. (d) D. R. van Staveren and N. Metzler-Nolte, *Chem. Rev*., 2004, **104**, 5931-5985.
21. N. D. Eljack, H.-Y. M. Ma, J. Drucker, C. Shen, T. W. Hambley, E. J. New, T. Friedrichb and R. J. Clarke, *Metallomics*, 2014, **6**, 2126-2133.
22. R. Mohammadi, R. Yousefi, M. D. Aseman, S. M Nabavizadeh and M. Rashidi, *Anticancer Agents Med. Chem.*, 2015, **15**, 107-114.
23. N. Cutillas, G. S. Yellol, C. de Haro, C. Vicente, V. Rodriguez and J. Ruiz, *Coord. Chem. Rev*., 2013, **257**, 2784-2797.
24. (a) X. Wang and Z. Guo, *Chem. Soc. Rev*., 2013, **42**, 202-224. (b) H. H.W. Chen and M. T. Kuo, *Met. Based Drugs*, 2010; article ID 430939.
25. (a) L. Zhao, Z. Wang, H. Wu, Z. Xi and Y. Liu, *Biochem. J.*, 2015, **472**, 217-223. (b) G. K. Balendiran, R. Dabur and D. Fraser, *Cell Biochem. Funct*., 2004, **22**, 343-352.
26. J. J. Soldevila-Barreda, I. Romero-Canelón, A. Habtemariam and P. J. Sadler, *Nat. Commun.*, 2015, **6**, 6582.
27. S. J. Dougan, M. Melchart, A. Habtemariam, S. Parsons and P. J. Sadler, *Inorg. Chem*., 2006, **45**, 10882-10894.
28. F. Ying, A. Habtemariam, A. M. Pizarro, S. H. van Rijt, D. J. Healey, P. A. Cooper, S. D. Shnyder, G. J. Clarkson, and P. J. Sadler, *J. Med. Chem*., 2010, **53**, 8192-8196.
29. P. Ghosh, S. Samanta, S. K Roy, S. Joy, T. Krämer, J. E. McGrady and S. Goswami, *Inorg. Chem*., 2013, **52**, 14040-14049.
30. S. J. Doughan, A. Habtemariam, S. E. McHale, S. Parsons and P. J. Sadler, *Proc. Natl. Acad. Sci. U.S.A.*, 2008, **105**, 11628-11633.
31. R. W. McDonald, W. Bunjobpon, T. Liu, S. Fessler, O. E. Pardo, I. K. Freer, M. Glaser, M. J. Seckl and D. J. Robins, *Anticancer Drug Des.*, 2001, **16**, 261-270.
32. (a) U. Basu, I. Khan, A. Hussain, P. Kondaiah and A. R. Chakravarty, *Angew. Chem. Int. Ed*., 2012, **51**, 2658-2661. (b) P. K. R. Nair, S. J. Melnick, S. F. Wnuk, M. Rapp, E. Escalon and C. Ramachandran, *J. Ethnopharmacol.*, 2009, **122**, 450-456.
33. A. Ali, D. Bansal, N. K. Kaushik, N. Kaushik, E. H. Choi, and R. Gupta, *J. Chem. Sci.*, 2014, **126**, 1091-1105.
34. N. Deibel, D. Schweinfurth, S. Hohloch, M. Delor, I. V. Sazanovich, M. Towrie, J. A. Weinstein, and B. Sarkar, *Inorg. Chem.*, 2014, **53**, 1021-1031. (b) S. Roy, I. Hartenbach and B. Sarkar, *Eur. J. Inorg. Chem.*, 2009, 2553-2558.
35. (a) A. Matsumoto, M. Suzuki, D. Kuzuhara, J. Yuasa, T. Kawai, N. Aratani and H. Yamada, *Chem. Commun.*, 2014, **50**, 10956-10958. (b) R. Haldar, K. Prasad, P. K. Samanta, S. Pati and T. K. Maji, *Cryst. Growth Des*., 2016, **16**, 82-91.
36. M. J. Frisch, *et al.* Gaussian 09, revision A.1; Gaussian, Inc.: Wallingford, CT, 2009 (see ESI† for full citation).
37. A. D. Becke, *Phys. Rev. A.*, 1988, **38**, 3098-3100.
38. A. D. Becke, *J. Chem. Phys*., 1993, **98**, 5648-5652.
39. (a) M. Ghedini, D. Pucci, A. Crispini and G. Barberio, *Organometallics*, 1999, **18**, 2116-2124. (b) M. Ghedini, T. Pugliese, M. L. Deda, N. Godbert, I. Aiello, M. Amati, S. Belviso, F. Lelj, G. Accorsi and F. Barigellettic, *Dalton Trans*., 2008, 4303-4318. (c) D. J. Mabbott, B. E. Mann and P. M. Maitlis, J. Chem. Soc., *Dalton Trans.*, 1977, 294-299.
40. (a) L. Salassa, H. I. A. Phillips and P. J. Sadler, *Phys. Chem. Chem. Phys*., 2009, **11**, 10311-10316. (b) I. Ritacco, E. M. Moustafa, E. Sicilia, N. Russoa and T. Shoeib, *Dalton Trans*., 2015, **44**, 4455-4467.
41. C. Garino and L. Salassa, *Philos. Trans. R. Soc., A*, 2013, **371**, 20120134.
42. S. S. Tan, S. J. Kim and E. T. Kool, *J. Am Chem Soc.*, 2011, **133**, 2664-2671.
43. H. Masuhara, H. Shioyama, T. Saito, K. Hamada, S. Yasoshima, and N. Mataga, *J. Phys. Chem.*, 1984, **88**, 5868-5873.
44. (a) M. T. Carter, M. Rodriguez and A. J. Bard, *J. Am. Chem. Soc.*, 1989, **111**, 8901-8911. (b) J. D. McGhee and P. H. von Hippel, *J. Mol. Biol.*, 1974, **86**, 469-489.
45. S. MoradpourHafshejani, J. H. Hedley, A. O. Haigh, A. R. Pike and E. M. Tuite, *RSC Adv*., 2013, **3**, 18164-18172.
46. B. Balaji, B. Balakrishnan, S. Perumalla, A. A. Karande and A. R. Chakravarty, *Eur. J. Med. Chem.*, 2015, **92**, 332-341.
47. D. Suh and J. B. Chaires, *Bioorg. Med. Chem.*, 1995, **3**, 723-728.
48. S. Saha, R. Majumdar, M. Roy, R. R. Dighe and A. R, Chakravarty, *Inorg. Chem.*, 2009, **48**, 2652-2663.
49. T. Mosmann, *J. Immunol Methods.*, 1983, **65**, 55-63.
50. J. Reedijk, *Eur. J. Inorg. Chem.*, 2009, 1303-1312.
51. B. Lippert, *Cisplatin, Chemistry and Biochemistry of a Leading Anticancer Drug*, Verlag Helvetica Chimica Acta: Zürich, Switzerland, 1999.
52. D. D. Perrin, W. L. F. Armarego and D. R. Perrin, *Purification of Laboratory Chemicals*, Pergamon Press, Oxford, 1980.
53. C. Zhang and N. Jiao, *Angew. Chem. Int. Ed*., 2010, **49**, 6174-6177.
54. D. F. Evans, *J. Chem. Soc.*, 1961, 1987-1993.
55. E. C. Taylor, G. H. Hawks and A. Mckillop, *J. Am. Chem. Soc.*, 1968, **90**, 2420-2421.

View Article Online
DOI: 10.1039/C6DT02500H

Table 1. Selected physicochemical data for the complexes **1**-**4**

Complex	**1**	**2**	**3**	**4**
^{1}H NMR $\gamma_{(C\text{-}H)}$ (ppm)[a]	5.95	6.20	5.97	5.51
IR (in KBr) $\nu_{C=O}$, $\nu_{N=N}$, cm^{-1}	1605, 1245	1602, 1255	1598, 1250	1612, 1250
Λ_M[b] / S m^2 M^{-1}	28	31	27	30
λ_{max} / nm (10^{-4} ε / dm^3 M^{-1} cm^{-1})[c]	430 (8.8), 365 (8.9)	540 (1.2), 381 (3.6)	390 (4.4), 365 (4.4)	524 (1.25), 412 (2.6)
λ_{em} / nm[d]	525	440	435	--
Φ[e]	0.017	0.058	0.045	--
E_f /V [ΔE_p /mV][f]	-0.89, -1.24 [80], -1.50	-0.88, -1.10 [80]	-0.84, -1.11 [95]	-0.80, -1.42
K_b[g] /M^{-1}	1.5(±0.3) x 10^4	7.5(±0.1) x 10^5	3.2(±0.3) x 10^5	1.2(±0.4) x 10^3

[a] In DMSO-d_6/$CDCl_3$ solutions. [b] Molar conductivity in DMF at 298K. [c] In 10% DMSO-DPBS. [d] Emission spectra in aq. DMSO (1:3 v/v) (λ_{ex} = 430 nm for **1**, 370 nm for **2** and 365 for **3**). [e] Quantum yield in aq. DMSO (1:3 v/v). Quantum yield measured using quinine sulphate in 1mM anthracene (Φ = 0.27) or fluorescien (Φ = 0.38) as standards. Error within ±5%. [f] Redox couple in DMF-0.1M TBAP. The potentials are vs. SCE. Scan rate = 100 mV s^{-1}. [g] Intrinsic equilibrium ct-DNA binding constant, K_b from UV-vis absorption spectral experiments.

Table 2. IC_{50} values of the complexes **1**-**4**, the ligands and related platinum complexes in HaCaT cells

Complexes	IC_{50} (μM) (Light)[a]	IC_{50} (μM) (Dark)[b]	Cellular uptake (ng Pt/10^6cells)[c]
1	10.9 ± 0.2	55.6 ± 0.6	2510
2	8.0 ± 0.3	45.0 ± 0.5	110
3	14.2 ± 0.5	61.9 ± 0.8	120
4	95.2 ± 1.1	>100	60
Hpy-acac	15.2 ± 0.8	>100	
An-acac	45.2 ± 1.4	>100	
Hcur	7.9± 0.4	23.2± 1.3	
Cisplatin		4.8± 0.7	
[Pt(pap)(an-cat)][d]	5.2 ± 0.1	57.0 ± 1.2	
$[Pt(cur)(NH_3)_2](NO_3)$[e]	15 ± 3	>200	
ttt-$[Pt(N_3)_2(OH)_2(NH_3)(py)]$[f]	6.1	>244.3	

[a] The IC_{50} values correspond to 4 h incubation in dark followed by 1 h photo-exposure to visible light of 400-700 nm (10 J cm^{-2}). [b] IC_{50} values correspond to 4 h incubation in dark. [c] In HaCaT cells on 4h incubation in dark. Pt content was estimated by ICPMS methods. [d] IC_{50} value taken from ref. 13. [e] IC_{50} value taken from ref. 14. [f] IC_{50} value in UVA light (365 nm) obtained from ref. 18a (*ttt*, *trans*,*trans*,*trans*).

Journal Name ARTICLE

Photoactive platinum(II) β-diketonates as dual action anticancer agents

View Article Online
DOI: 10.1039/C6DT02590K

Md Kausar Raza[a,#], Koushambi Mitra[a,#], Abhijith Shettar[b], Uttara Basu[a], Paturu Kondaiah*[,b] and Akhil R. Chakravarty*[,a]

Keywords: Bioinorganic chemistry, platinum, β-diketonates, curcumin, photocytotoxicity.

Synopsis (20 words): Cyclometallated platinum(II) β-diketonates show significant photocytotoxicity in skin-keratinocyte HaCaT cells [IC_{50}: ~10 μM (visible light, 400-700 nm), ≥60 μM (dark)].

Pictogram: